ISSN 0967-0912, Steel in Translation, 2018, Vol. 48, No. 4, pp. 229–232. © Allerton Press, Inc., 2018.
Original Russian Text © V.E. Gromov, V.E. Kormyshev, A.M. Glezer, S.V. Konovalov, Yu.F. Ivanov, 2018, published in Izvestiya Vysshikh Uchebnykh Zavedenii, Chernaya Metallurgiya, 2018, No. 4, pp. 313–318.

Gradient Structure of the Layer Applied to Hardox 450 Steel by Fe–C– Cr–Nb–W Powder Wire after Electron-Beam Treatment

V. E. Gromov[a, *], V. E. Kormyshev[a, **], A. M. Glezer[b, *], S. V. Konovalov[c, ****], and Yu. F. Ivanov[d, e, *****]**

[a] *Siberian State Industrial University, Novokuznetsk, 654007 Russia*
[b] *Bardin Central Research Institute of Ferrous Metallurgy, Moscow, 105005 Russia*
[c] *Samara National Research University, Samara, 443086 Russia*
[d] *Institute of High-Current Electronics, Siberian Branch, Russian Academy of Sciences, Tomsk, 634055 Russia*
[e] *Tomsk State University, Tomsk, 634050 Russia*
**e-mail: gromov@physics.sibsiu.ru*
***e-mail: 89236230000@mail.ru*
****e-mail: aglezer@mail.ru*
*****e-mail: ksv@ssau.ru*
******e-mail: yufi55@mail.ru*

Received December 15, 2016

Abstract—Surfacing with composite coatings strengthened by carbide, boride, and other particles is currently of great interest in materials physics. The performance of the applied layer is primarily determined by the phase composition of the coating. To permit the selection of coatings capable of withstanding extremal operating conditions, including high loads and abrasive wear, their properties and structure must be investigated in detail. In the present work, state-of-the-art techniques in materials physics are used to study the structure, phase composition, and tribological properties of coatings applied to Hardox 450 low-carbon martensitic steel by Fe–C– Cr–Nb–W powder wire and then subjected to electron-beam treatment. The electron-beam parameters are as follows: in the first stage, energy density per pulse $E_S = 30$ J/cm^2; pulse length $\tau = 200$ μs; and number of pulses $N = 20$; in the second stage, $E_S = 30$ J/cm^2; $\tau = 50$ μs; and $N = 1$. These conditions are selected on the basis of calculations of the temperature field formed in the surface layer of the material by a single pulse. It is found that electron-beam treatment of an applied layer of thickness about 5 mm leads to modification of a thin surface layer (about 20 μm), consisting largely of α iron and the carbide NbC; small quantities of the carbides Fe_3C and Me_6C (Fe_3W_3C) are also present. This modified surface layer differs from the unmodified coating mainly in terms of the morphology and dimensions of the secondary-phase inclusions. In the modified surface layer, the inclusions are smaller and take the form of thin layers along the grain boundaries. In the unmodified coating, the inclusions are mainly rounded particles, chaotically distributed within the grain. After electron-beam treatment, the wear resistance of the applied layer increases by a factor greater than 70 with respect to Hardox 450 steel, while the frictional coefficient is significantly less (about a third as much).

Keywords: surfacing, metal structure, phase composition, electron-beam treatment, morphology, hard carbides, tribological properties

DOI: 10.3103/S0967091218040034

Globally, billions of dollars are lost each year on account of the wear and corrosion of machine parts and structures. The main approach to preventing wear and corrosion, until recently, was bulk alloying, but the reserves of alloying elements are being exhausted and their cost is increasing considerably.

In recent years, research interest has turned to surfacing with composite coatings strengthened by carbide, boride, and other particles [1–7]. Such coatings prove effective in the presence of strong abrasive wear and impact loads and are widely used in industry. Their performance largely depends on their chemical and phase composition [8–11]. To permit the selection of coatings best suited to particular operating conditions, their properties and structure must be investigated in detail [12–16].

Effective use of surfacing entails careful analysis of the relation between wear, hardness, and microstruc-

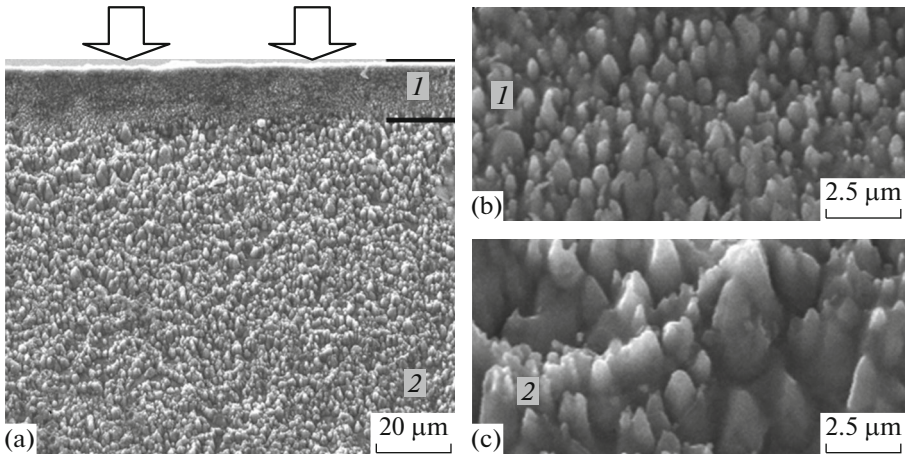

Fig. 1. Structure of the applied layer transverse to the etched section after electron-beam treatment (at the surface indicated by the arrows): (*1*) modified surface layer; (*2*) unmodified coating.

ture [17–20]. That is essential to the production of components with high performance.

In the present work, state-of-the-art techniques in materials physics are used to study the structure, phase composition, and tribological properties of coatings applied to Hardox 450 low-carbon martensitic steel by electrocontact surfacing with Fe–C–Cr–Nb–W powder wire and then subjected to electron-beam treatment.

The composition of Hardox 450 steel is as follows: 0.19–0.26 wt % C, 0.70 wt % Si, 1.6 wt % Mn, 0.025 wt % P, 0.010 wt % S, 0.25 wt % Cr, 0.25 wt % Ni, 0.25 wt % Mo, and 0.004 wt %. The balance is iron. Because its content of alloying elements is low, Hardox 450 steel is relatively easy to weld and machine. The heat treatment of the steel consists of rapid cooling of the rolled sheets without subsequent tempering. That results in fine-grain structure and high levels of hardness. The steel is resistant to most forms of wear.

A strengthening layer is applied by arc welding with a floating metal electrode in an inert/active gas medium, with automatic supply of the powder wire in protective gas (98% Ar, 2% CO_2) [21]. The welding current is 250–300 A and the voltage is 30–35 V. The surfacing electrode is powder wire (diameter 1.6 mm) with the following composition: 1.3 wt % C, 7.0 wt % Cr, 8.5 wt % Nb, 1.4 wt % W, 0.9 wt % Mn, and 1.1 wt % Si. The balance is iron. A high-strength surface layer of thickness around 5 mm is formed.

To improve the tribological properties of the applied layer, it is modified by electron-beam treatment on a SOLO system, with melting and fast solidification [22]. The electron-beam parameters are as follows: in the first stage, energy density per pulse E_S = 30 J/cm^2; pulse length τ = 200 μs; and number of pulses N = 20; in the second stage, E_S = 30 J/cm^2; τ = 50 μs; and N = 1. These conditions are selected on the basis of calculations of the temperature field formed in the surface layer of the material by a single pulse [23]. The modified surface is tested on a CSEM high-temperature S/N 07-142 tribometer (CSEM Instruments); the counterbody is a ball (diameter 2 mm) of VK6 hard alloy. The wear rate is estimated from the cross-sectional area of the wear track, by means of a STIL Micro Measure 3D station. The structure of the modified layer is analyzed by means of transverse sections. To that end, the samples are cut in two perpendicularly to the modified surface.

The defect structure is studied by optical microscopy (on a μVizo Met-221 metallographic instrument), scanning electron microscopy (on a SEM-515 Philips instrument), and transmission diffraction electron microscopy (on EM-125 and FEI Tecnai 20 G2 Twin instruments). The elemental composition of the surface layer is determined by X-ray microspectral analysis, using the EDAX ECON IV attachment to the SEM-515 Philips scanning electron microscope. The phase composition of the surface layer is analyzed by X-ray diffraction on an XRD-7000s instrument (Shimadzu, Japan).

Electron-beam treatment of the applied layer leads to modification of a thin surface layer (about 20 μm) (Fig. 1a). This modified surface layer differs from the unmodified coating mainly in terms of the structure observed on ionic etching of a transverse section.

In the modified surface layer, the structural elements observed in etching (which are obviously refractory compounds that are poorly etched by the ion beam) measure 150–750 nm (Fig. 1b). Within the unmodified coating, the etched structural elements measure 1.5 μm (Fig. 1c).

In Fig. 2, we show typical images of the modified surface layer after electron-beam treatment (transmission electron microscopy). It is clear that the α phase has a plate structure and is formed as a result of $\gamma \rightarrow \alpha$ transition. The inclusions of secondary phase (indi-

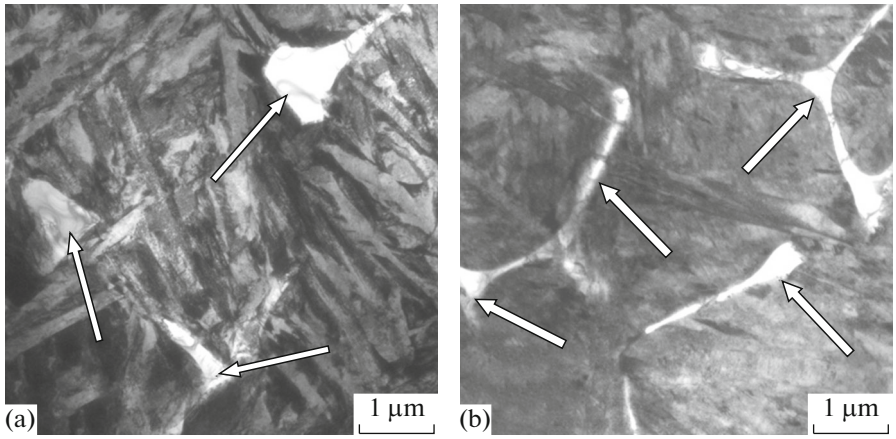

Fig. 2. Typical images of the structure of the modified surface layer after electron-beam treatment (transmission electron microscopy). The arrows indicate inclusions of secondary phase.

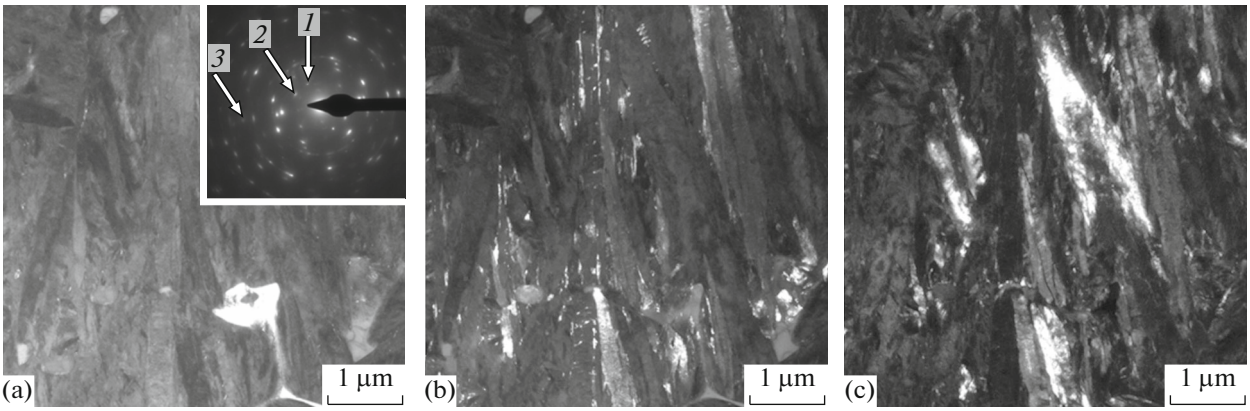

Fig. 3. Electron-microscopic images of the structure of the applied layer after electron-beam treatment: (a–c) dark-field images obtained in the reflexes [511] Me_6C (Fe_3W_3C), [110] α Fe + [102] Fe_3C, and [024] α Fe, respectively. Arrows *1–3* in the inset show the reflexes used for images (a)–(c), respectively.

cated by arrows in Fig. 2) take the form of thin layers (thickness 100–150 nm) along the grain boundaries. The inclusions at grain junctions are three-legged figures measuring up to 1 μm.

By dark-field microdiffraction analysis, we find that the inclusions of secondary phase in the form of thin layers along the grain boundaries consist of the carbide (Me_6C (Fe_3W_3C) (Fig. 3a). Within the martensite grains and along their boundaries, we see particles of iron carbide Fe_3C or possibly Me_3C (Fig. 3b).

The structure of the modified surface layer is characterized by the presence of faceted niobium-carbide inclusions, chaotically distributed within the grains. These inclusions measure 2 μm.

Thus, by electron diffraction microscopy, we find that the modified surface layer of the applied coating consists of many phases, most notably a solid solution based on α iron and the carbides Me_6C, NbC, and Fe_3C.

In the unmodified coating at a distance of 5 mm from the surface, faceted niobium carbides are the primary inclusions.

After electron-beam treatment, the basic difference between this modified surface layer and the unmodified coating concerns the morphology and dimensions of the inclusions of secondary phases. In the modified surface layer, the inclusions are smaller and take the form of thin layers along the grain boundaries. In the unmodified coating, the inclusions are mainly rounded particles, chaotically distributed within the grain.

After electron-beam treatment, the wear resistance of the applied layer increases by a factor greater than 70 with respect to Hardox 450 steel, while the frictional coefficient is about a third of that of the steel.

CONCLUSIONS

We have investigated the structure, phase composition, and tribological properties of coatings applied to

Hardox 450 low-carbon martensitic steel by Fe–C–Cr–Nb–W powder wire and then subjected to electron-beam treatment.

Surface treatment of the applied coating by electron-beam pulses reduces the size of the structural elements in a thin surface layer and changes the morphology of the carbide phase. As a result, the wear resistance is significantly improved and the frictional coefficient is decreased.

ACKNOWLEDGMENTS

Financial support was provided by the Russian Science Foundation (project no. 15-19-00065).

REFERENCES

1. Mendez, P.F., Barnes, N., Bell, K., Borle, S.D., Gajapathi, S.S., Guest, S.D., Izadia, H., Gola, A.K., and Wood, G., Welding processes for wear resistant overlays, *J. Manuf. Process.*, 2014, vol. 16, pp. 4–25.
2. Thorpe, W.R. and Chicco, B., On the formation of duplex eutectic carbides in commercially important white irons, *Mater. Sci. Eng.*, 1981, vol. 51, pp. 11–19.
3. Randle, V. and Laird, G., Microtexture study of eutectic carbides in white cast iron using electron backscatter diffraction, *J. Mater. Sci.*, 1993, vol. 28, pp. 4245–4249.
4. Pearce, J.T.H. and Elwell, D.W.L., Duplex nature of eutectic carbides in heat-treated 30% chromium cast iron, *J. Mater. Sci. Lett.*, 1986, vol. 5, pp. 1063–1064.
5. Wiengmoon, A., Chairuangsri, T., Brown, A., Brydson, R., Edmonds, D.V., and Pearce, J.T.H., Microstructural and crystallographical study of carbides in 30 wt % Cr cast irons, *Acta Mater.*, 2005, vol. 53, pp. 4143–4154.
6. Chen, X., Shen, Z., Chen, X., Lei, Y., and Huang, Q., Corrosion behavior of CLAM steel weldment in flowing liquid Pb–17Li, at 480°C, *Fusion Eng. Des.*, 2011, vol. 86, no. 12, pp. 2943–2948.
7. Chen, X., Fang, Y., Li, P., Yu, Z., Wu, X., and Li, D., Microstructure, residual stress and mechanical properties of a high strength steel weld using low transformation temperature welding wires, *Mater. Des.*, 2015, vol. 65, pp. 1214–1221.
8. Konovalov, S.V., Kormyshev, V.E., Ivanov, Yu.F., and Teresov, A.D., Electron-beam processing of the hardened layer formed on Hardox 450 steel electric-wire welding system Fe–C–V–Cr–Nb–W, *Letters on Materials*, 2016, vol. 6, no. 4, pp. 350–354.
9. Márquez-Herrera, A., Fernandez-Muñoz, J.L., Zapata-Torres, M., et al., Fe_2B coating on ASTM A-36 steel surfaces and its evaluation of hardness and corrosion resistance, *Surf. Coat. Technol.*, 2014, vol. 254, pp. 433–439.
10. Zahiri, R., Sundaramoorthy, R., Lysz, P., and Subramanian, C., Hardfacing using ferroalloy powder mixtures by submerged arc welding, *Surf. Coat. Technol.*, 2014, vol. 260, pp. 220–229.
11. Li, R., Zhou, Z., He, D., et al., Microstructure and high temperature corrosion behavior of wire-arc sprayed FeCrSiB coating, *J. Therm. Spray Technol.*, 2015, vol. 24, no. 5, pp. 857–864.
12. Kapralov, E.V., Raikov, S.V., Budovskikh, E.A., Gromov, V.E., Vaschuk, E.S., and Ivanov, Yu.F., Structural phase states and properties of coatings welded onto steel surfaces using powder, *Bull. Russ. Acad. Sci.: Phys.*, 2014, vol. 78, no. 10, pp. 1015–1021.
13. Gromov, V.E., Kapralov, E.V., Raikov, S.V., Ivanov, Yu.F., and Budovskikh, E.A., Structure and properties of wear-resistant coatings deposited by electric arc method on steel with flux cored wires, *Usp. Fiz. Met.*, 2014, vol. 15, no. 4, pp. 213–234.
14. Konovalov, S.V., Kormyshev, V.E., Gromov, V.E., Ivanov, Yu.F., Kapralov, E.V., and Semin, A.P., Formation features of structure-phase states of Cr–Nb–C–V containing coatings on martensitic steel, *J. Surf. Investig.*, 2016, vol. 10, no. 5, pp. 1119–1124.
15. Berns H. and Fischer A., Microstructure of Fe–Cr–C hardfacing alloys with additions of Nb, Ti and B, *Mater. Charact.*, 1997, vol. 39, pp. 499–527.
16. Berns, H. and Fischer, A., Abrasive wear resistance and microstructure of Fe–Cr–C–B hard surfacing weld deposits, *Wear*, 1986, vol. 112, no. 2, pp. 163–180.
17. Yüksel, N. and Şahin, S., Wear behavior–hardness–microstructure relation of Fe–Cr–C and Fe–Cr–C–B based hardfacing alloys, *Mater. Des.*, 2014, vol. 58, pp. 491–498.
18. Venkatesh, B., Sriker, K., and Prabhakar, V.S.V., Wear characteristics of hardfacing alloys: state-of-the-art, *Proc. Mater. Sci.*, 2015, vol. 10, pp. 527–532.
19. Gualco A., Marini C., Svoboda H., and Surian E., Wear resistance of Fe-based nanostructured hardfacing, *Proc. Mater. Sci.*, 2015, vol. 8, pp. 934–943.
20. Teker, T., Karatas, S., and Osman Yilmaz, S., Microstructure and wear properties of AISI 1020 steel surface modified by HARDOX 450 and FeB powder mixture, *Prot. Met. Phys. Chem. Surf.*, 2014, vol. 50, no. 1, pp. 94–103.
21. Malysh, V.M. and Soroka, M.M., *Elektricheskaya svarka* (Electric Welding), Kiev: Tekhnika, 1986.
22. Koval', N.N. and Ivanov, Yu.F., Nanostructuring of surfaces of metalloceramic and ceramic materials by electron-beams, *Russ. Phys. J.*, 2008, vol. 51, no. 5, pp. 505–516.
23. *Evolyutsiya struktury poverkhnostnogo sloya stali, podvergnutoi elektronno-ionno-plazmennym metodam obrabotki* (Evolution of Structure of the Surface Layer of Steel Treated by Electron-Ion-Plasma Methods), Koval', N.N. and Ivanov, Yu.F., Eds., Tomsk: Izd. Nauchno-Tekh. Lit., 2016.

Translated by Bernard Gilbert